

# ChemComm

Accepted Manuscript



This is an *Accepted Manuscript*, which has been through the Royal Society of Chemistry peer review process and has been accepted for publication.

*Accepted Manuscripts* are published online shortly after acceptance, before technical editing, formatting and proof reading. Using this free service, authors can make their results available to the community, in citable form, before we publish the edited article. We will replace this *Accepted Manuscript* with the edited and formatted *Advance Article* as soon as it is available.

You can find more information about *Accepted Manuscripts* in the [Information for Authors](#).

Please note that technical editing may introduce minor changes to the text and/or graphics, which may alter content. The journal's standard [Terms & Conditions](#) and the [Ethical guidelines](#) still apply. In no event shall the Royal Society of Chemistry be held responsible for any errors or omissions in this *Accepted Manuscript* or any consequences arising from the use of any information it contains.

## COMMUNICATION

# Multistimuli-responsive azobenzene nanofibers with aggregation-induced emission enhancement characteristics

Cite this: DOI: 10.1039/x0xx00000x

Received 00th January 2012,

Accepted 00th January 2012

DOI: 10.1039/x0xx00000x

www.rsc.org/

Mina Han,<sup>\*a</sup> Sung June Cho,<sup>\*b</sup> Yasuo Norikane,<sup>c</sup> Masaki Shimizu,<sup>d</sup> Akinori Kimura,<sup>d</sup> Tomokazu Tamagawa,<sup>d</sup> and Takahiro Seki<sup>a</sup>

**A new azobenzene-based chromophore was synthesized to create one-dimensional (1D) nanofibers with aggregation-induced emission enhancement characteristics. The enhanced red fluorescence of the fibrous structures can be switched off via mechanical pressure, friction, or heat by pressing, rubbing, or annealing.**

Diverse nano/microstructures and their unique functions can be realized by delicately modulating the nature of organic compounds and their spatial arrangements. Design and creation of smart fluorescent materials capable of switching their fluorescence intensity and/or color in response to light, heat, friction and mechanical pressure have much attention due to their applications in optoelectronic devices, information storage, sensor, and actuators.<sup>1,2</sup>

Azobenzene is a widely used photochromic compound, but it is known as a *non-fluorescent chromophore* (with a quantum yield  $\Phi_f \approx 10^{-7}$ – $10^{-5}$ ).<sup>3</sup> Nevertheless, very weak fluorescence has occasionally been detected from azobenzene derivatives in the following categories: (i) donor-acceptor substituted azobenzenes,<sup>4</sup> (ii) *o*- and *p*-hydroxy azo compounds,<sup>5</sup> (iii) azobenzenes with bulky *ortho* substituents,<sup>6</sup> (iv) *trans*-blocked azobenzenes,<sup>7</sup> (v) self-assembled aggregates<sup>8,9</sup> (i.e., aggregation-induced emission enhancement [AIEE]<sup>10</sup>). AIEE is the opposite of aggregation-caused quenching that conventional  $\pi$ -conjugated organic fluorophores commonly experience. Restriction of intramolecular rotation,<sup>10a,10d</sup> aggregation-induced planarization and head-to-tail molecular arrangement<sup>10b,10c</sup> are associated with the enhanced emission in the aggregated state. The number of AIEE-active azobenzene-based chromophores is exceedingly limited.<sup>8,9</sup> Shimomura and Kunitake demonstrated that fluorescence at 600 nm is detected from azobenzene-containing bilayer membranes in which the transition dipoles of the azobenzene chromophores are aligned in a head-to-tail fashion.<sup>8a</sup> Han *et al.* recently described that linear azobenzenes with long alkyl chains slowly assemble into intensely fluorescent aggregates under UV light illumination.<sup>9a,9b</sup> Self-assembled spheres<sup>9a,9b</sup> and microrods<sup>8c</sup> composed of azobenzene chromophores are sufficiently fluorescent to be visualized by fluorescence optical microscopy. However, neither the elucidation of the underlying mechanism nor the design of multistimuli-responsive fluorescent azobenzenes has still been successfully achieved. Here we describe

fluorescent one-dimensional (1D) nanofibers generated via the self-assembly of new azobenzene-based chromophores. The crystalline fiber formation was accompanied by a significant red shift in the absorption bands and an approximately fourfold increase in fluorescence efficiency. Combining our experimental results with Rietveld refinement and density functional theory (DFT) calculations we provide important information on the molecular arrangement that determines not only the 1D molecular assembly but also the AIEE features. Interestingly, the red fluorescence of the crystalline fibers can readily be switched off by pressing, rubbing, or annealing.

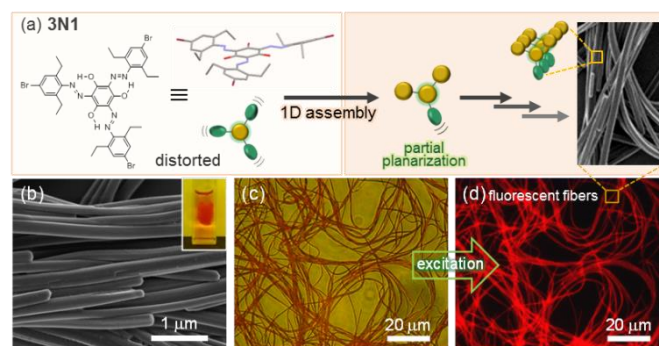


**Fig. 1** (a) Chemical and optimized **3N1** structure using B3LYP/6-31G(d), and schematic representation of the 1D assembly. (b) SEM, (c) OM and the corresponding (d) FOM ( $\lambda_{\text{ex}} = 520$ – $550$  nm) images of 1D nanofibers (see also Fig. S4). The inset photograph in Fig. 1b shows a largely entangled **3N1** agglomerate.

Taking into account a balance of steric constraints, hydrogen bonding, and  $\pi$ - $\pi$  stacking interactions, we synthesized a trigonal azobenzene derivative (**3N1**, Fig. 1a and Supporting Information), in which three phenyl rings are connected to a central 1,3,5-trihydroxybenzene core via azo ( $-\text{N}=\text{N}-$ ) groups. Due to the sterically crowded 4-bromo-2,6-diethylphenyl groups, the central aromatic core cannot be coplanar with the three surrounding aromatic rings, as supported by DFT calculations (Fig. S3). The simple trigonal compound tends to assemble into crystalline 1D

structures (cylindrical rods and/or fibers)<sup>11</sup> due to the balance between the steric constraints from the three surrounding aromatic rings and noncovalent interactions such as hydrogen bonding and  $\pi$ - $\pi$  stacking.

To prepare the 1D structures, we added water to a **3N1** tetrahydrofuran (THF) solution with gentle stirring. The THF/H<sub>2</sub>O solution became opaque with increasing water content. Subsequently tiny red floaters observable with the naked eye formed. Stirring for several more seconds yielded a largely entangled agglomerate, which eventually separated from the transparent solvent mixture (inset photograph in Fig. 1b).

We examined the aggregation behavior by taking aliquots of the entangled agglomerates and characterizing their shape and size by scanning electron microscopy (SEM), optical microscopy (OM), and fluorescence optical microscopy (FOM) observations. The SEM images in Fig. 1b and Fig. S4 contain fibrous structures that are approximately 100–200 nm thick and over several tens of micrometers long. Even at higher concentrations, the elongated nanofibers were relatively uniform in their thickness and did not fuse to one another to produce thicker structures (e.g., micrometer- or macrometer-sized). Notably, the FOM image (Fig. 1d) corresponding to the OM image shown in Fig. 1c reveals that the fibers can easily be identified by their red fluorescence when excited with green light.

Regardless the excitation wavelength (460–520 nm), **3N1** in THF solution exhibits weak fluorescence at around 560 nm (with a fluorescence quantum yield of 0.002).<sup>12</sup> Importantly, the formation of nanofibers by addition of water to the **3N1** solution (THF/H<sub>2</sub>O = 1/1, v/v) increases the fluorescence intensity together with a noticeable red shift of the maximum wavelength to 608 nm (Fig. 2a). The absolute fluorescence quantum yield of the dried fibers was 0.008, which is four times higher than that of the THF solution. This increased fluorescence efficiency confirms that **3N1** is AIEE-active.

Fig. 2b shows the absorption spectral changes before and after the formation of the 1D fibers. The absorption band centered at 362 nm is attributed to a  $\pi$ - $\pi^*$  transition of the azobenzene unit. The stronger band at 476 nm presumably originates from the energetic proximity of the ( $\pi$ , $\pi^*$ ) and ( $n$ , $\pi^*$ ) states not only due to the charge transfer character of donor-acceptor substituted azobenzene, but also due to intramolecular O—H...N hydrogen bonding interactions (Fig. S3).<sup>3</sup> In addition, the forbidden  $n$ - $\pi^*$  transition for planar *trans*-azobenzene becomes partially allowed for distorted *trans*-azobenzene, which increases the molar extinction coefficient.<sup>3,13</sup> After the formation of the 1D fibers, the  $\pi$ - $\pi^*$  absorption band is remarkably red-shifted to 382 nm. A shoulder also appears in the 545–565 nm range. We infer from these spectral changes that the

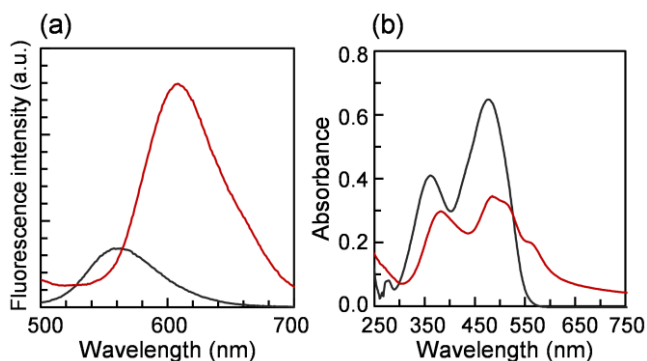


**Fig. 2** Changes in (a) fluorescence (excitation at 460 nm) and (b) UV-vis absorption spectra before ( $2 \times 10^{-5}$  M in THF, black line) and after (red line) formation of 1D fibers ( $2 \times 10^{-5}$  M THF/H<sub>2</sub>O [1/1, v/v]).

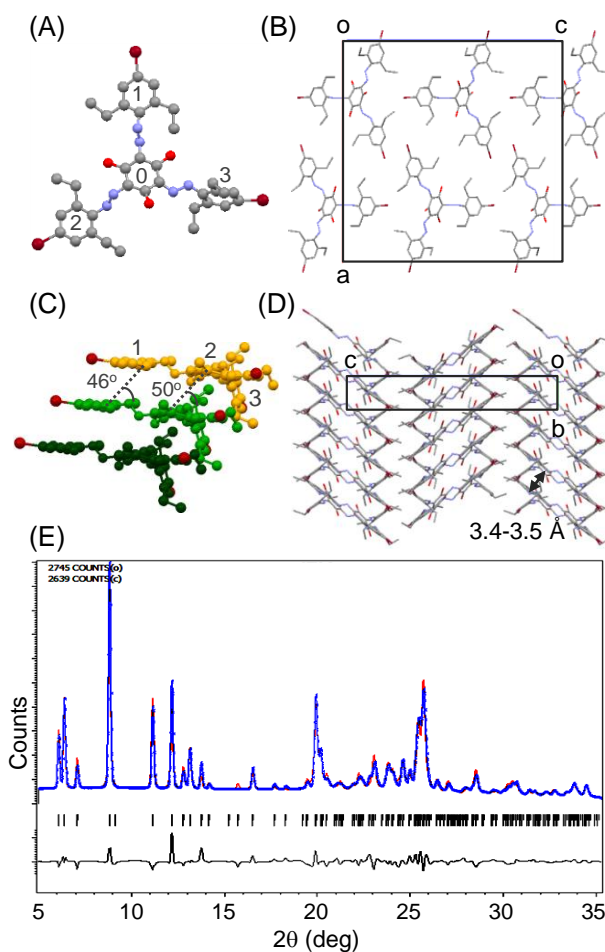


**Fig. 3** (A) **3N1** adopts a partially planar conformation in a crystalline fiber, based on the Rietveld refinement of the XRD pattern for the fibers (Fig. 3E). (B) Molecular packing diagram viewed along the *b* axis. (C) Packing structure. (D) Packing diagram viewed along the *a* axis. **3N1** molecules are regularly packed along the *b* direction. (E) Rietveld refinement patterns for the fibers using XRD data at ambient temperature. The observed X-ray diffraction pattern (blue solid line) was compared to the calculated XRD pattern (red solid line) with the difference plot (black solid line). The Bragg positions are shown as black bars

**3N1** molecules would be packed in an inclined fashion (i.e., J-aggregation),<sup>14</sup> which is supported by hydrogen bonding and  $\pi$ - $\pi$  stacking interactions between the aromatic rings.

To understand the molecular arrangement responsible for the 1D molecular assembly and enhanced emission characteristics, we performed Rietveld refinement of the X-ray diffraction (XRD) pattern for the freshly prepared fibers. The Rietveld analysis exhibits the good fitting quality ( $R_p = 6.7\%$ ,  $R_{wp} = 9.2\%$ , and  $GOF = 1.47$ ),<sup>15</sup> as shown in Fig. 3E and Fig. S6. Interestingly, the **3N1** molecule in the crystalline fiber adopts a distinctive conformation: One phenyl ring (3 in Fig. 3A) lies out of the central aromatic core plane (0 in Fig. 3A). The two phenyl rings (0 and 3) are twisted by  $\sim 79^\circ$  from planarity. Considering the distorted X-ray crystal structure for *ortho*-diethylated azobenzene (with a torsion angle of  $68^\circ$ ),<sup>16</sup> such a high distortion seems acceptable. In sharp contrast, the remaining two phenyl rings (1 and 2 in Fig. 3A) become somewhat coplanar with the central aromatic core, although each phenyl ring (0, 1, and 2)

maintains a split-level structure with respect to the azo group (Fig. 3C).

The molecular packing illustrations (Fig. 3C and 3D) depict that the respective **3N1** molecules have a mutually inclined arrangement with interlayer distances of 3.48 and 3.46 Å ( $2\theta = 25.52$  and  $25.66^\circ$ , respectively, see the XRD data in Fig. 3E), which forms cylindrical structures via  $\pi$ - $\pi$  stacking interactions. The partially planar **3N1** molecules are inclined with tilt angles of  $46^\circ$  and  $50^\circ$ . Both the conformational transformation from the distorted trigonal to partially planar form and the inclined molecular arrangement<sup>17</sup> lead to a red shift in the  $\pi$ - $\pi^*$  absorption band and an increase in the fluorescence efficiency.

We next hypothesized that, if the red fluorescence enhancement is indeed due to the formation of the crystalline fibers, the fluorescence should be switched off by reducing the degree of crystallinity. To test this hypothesis, we simply pressed (or rubbed) the entangled fibers with a metal spatula. Amazingly, the color changed from dark red to bright red and the fluorescence intensity was noticeably reduced in the pressed (or rubbed) region, as clearly shown in OM and FOM images, respectively (Fig. 4).

In addition to mechanical pressure and friction, annealing of the crystalline fibers above the melting temperature lowered the fluorescence intensity and eventually the red fluorescence almost disappears (Fig. 4c and Fig. S7). As expected from the previous reports,<sup>2</sup> such external stimuli could probably alter the degree of

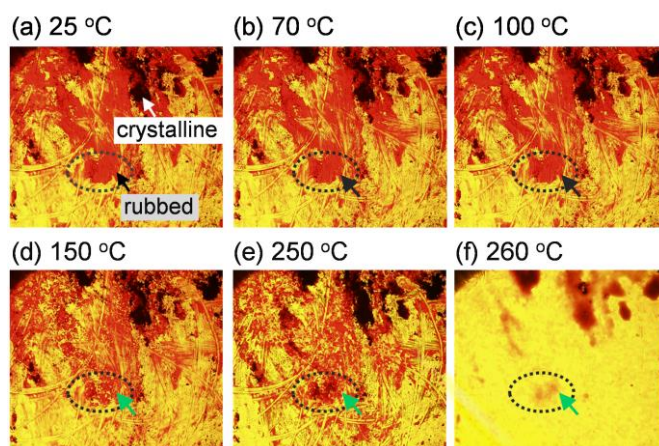


Fig. 5 OM images taken as a function of annealing temperature..

intermolecular interactions and spatial arrangements of the individual components. Fig. 5 displays that the rubbed samples is not crystalline but rather an amorphous sticky paste, which suggests a possibly random molecular arrangement. The OM images taken as a function of annealing temperature offer direct evidence that the morphology of the rubbed samples begins changing near  $150^\circ\text{C}$ , and they become liquid at  $260^\circ\text{C}$ , unlike the crystalline fibers that melt at  $260^\circ\text{C}$ . Thus these results indicate that the fiber crystallinity decreases due to the mechanical pressure, friction and heat caused by pressing, rubbing and thermal treatment, which alters the color and fluorescence intensity. The multistimuli-induced “fluorescence off” state reverts to the original state upon solvent-induced self-assembly.

In summary, we have demonstrated red fluorescent 1D structures generated via the self-assembly of a new AIEE-active azobenzene chromophore. The combination of our spectroscopic results, DFT calculations, and the Rietveld refinement of the XRD data for the crystalline nanofibers reveals that the partially increased planarization and inclined arrangements of the chromophores are responsible for the red shift in the absorption bands and the increase in the fluorescence efficiency. The enhanced red fluorescence for the fibrous structures can be switched off by pressing, rubbing, or annealing. Our findings may be applicable to the development of stimuli-responsive luminescent materials that range from optoelectronic devices and sensors to fluorescent polarizers combined with unidirectional molecular arrangements in polymeric objects.

## Acknowledgements

We are grateful to Prof. Ja-Hyoung Ryu (UNIST, Korea) for helpful discussions as well as to Dr. Tatsuo Hikage and Dr. Mitsuo Hara (Nagoya University) for their assistance with the XRD experiments.

## Notes and references

<sup>a</sup> Department of Molecular Design & Engineering, Nagoya University, Furo-cho, Chikusa-ku, Nagoya 464-8603, Japan.

E-mail: hanmin@apchem.nagoya-u.ac.jp

<sup>b</sup> Department of Applied Chemical Engineering, Chonnam National University, Yongbong 300, Buk-gu, Gwangju 500-757, Korea.

E-mail: sjcho@chonnam.ac.kr

<sup>c</sup> Electronics and Photonics Research Institute, National Institute of Advanced Industrial Science and Technology (AIST), Central 5, Higashi 1-1-1, Tsukuba, Ibaraki 305-8565, Japan

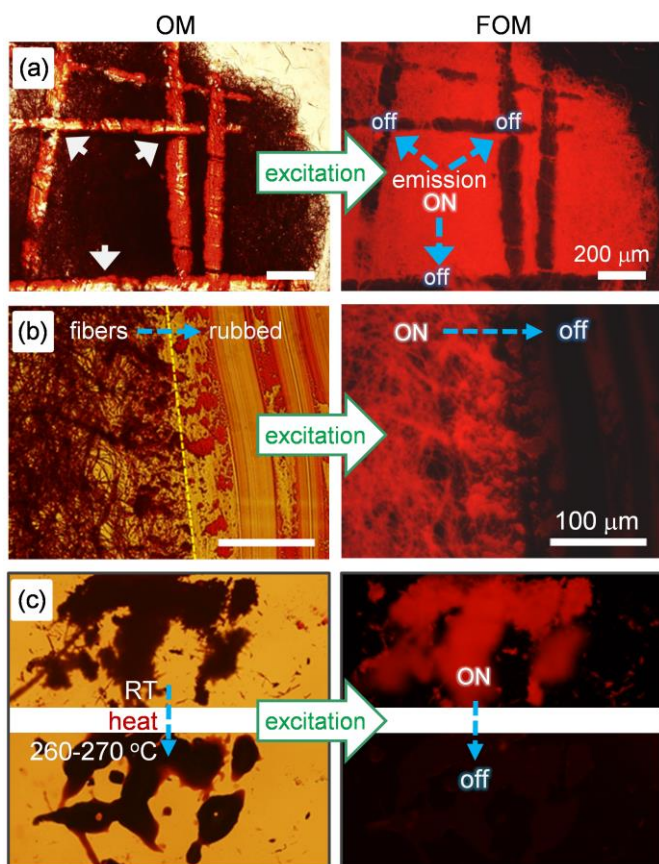


Fig. 4 (Left) OM and the corresponding (right) FOM images of crystalline fibers (a) pressed (see white arrows) and (b) rubbed with a metal spatula. The color change and fluorescence intensity reduction were clearly seen in the pressed and rubbed regions. (c) OM and the corresponding FOM images taken at (upper) room temperature and (lower)  $260$ – $270^\circ\text{C}$  (also see Fig. S7).

<sup>d</sup> Department of Biomolecular Engineering, Graduate School of Science and Technology, Kyoto Institute of Technology, 1 Hashikami-cho, Matsugasaki, Sakyo-ku, Kyoto 606-8585, Japan

<sup>†</sup> Electronic Supplementary Information (ESI) available: [Experimental and characterization details, growth process, optimized **3N1** structure using B3LYP/6-31G(d), FT-IR absorption spectrum, OM images taken as a function of annealing temperature, data collection and crystallographic parameters for **3N1**, atomic coordinates and displacement and population parameters for **3N1**]. See DOI: 10.1039/c000000x/

- 1 (a) C. W. Tang, S. A. VanSlyke and C. H. Chen, *Appl. Phys. Lett.*, 1987, **51**, 913; (b) C. Adachi, T. Tsutsui and S. Saito, *Appl. Phys. Lett.*, 1990, **56**, 799; (c) A. P. de Silva, H. Q. N. Gunaratne, T. Gunnlaugsson, A. J. M. Huxley, C. P. McCoy, J. T. Rademacher and T. E. Rice, *Chem. Rev.*, 1997, **97**, 1515; (d) D. T. McQuade, A. E. Pullen and T. M. Swager, *Chem. Rev.*, 2000, **100**, 2537; (e) S. R. Forrest, *Nature*, 2004, **428**, 911; (f) S. J. Toal, K. A. Jones, D. Magde and W. C. Trogler, *J. Am. Chem. Soc.*, 2005, **127**, 11661; (g) P. Bosch, F. Catalina, T. Corrales and C. Peinado, *Chem.-Eur. J.*, 2005, **11**, 4314; (h) D. Knapton, M. Burnworth, S. J. Rowan and C. Weder, *Angew. Chem. Int. Ed.*, 2006, **45**, 5825; (i) A. Pucci, F. Di Cuia, F. Signori and G. Ruggeri, *J. Mater. Chem.*, 2007, **17**, 783.
- 2 (a) Y. Sagara, T. Mutai, I. Yoshikawa and K. Araki, *J. Am. Chem. Soc.*, 2007, **129**, 1520; (b) J. Kunzelman, M. Kinami, B. Crenshaw, J. Protasiewicz and C. Weder, *Adv. Mater.*, 2008, **20**, 119; (c) H. Ito, T. Saito, N. Oshima, N. Kitamura, S. Ishizaka, Y. Hinatsu, M. Wakeshima, M. Kato, K. Tsuge and M. Sawamura, *J. Am. Chem. Soc.*, 2008, **130**, 10044; (d) Y. Sagara and T. Kato, *Nat. Chem.*, 2009, **1**, 605; (e) G. Zhang, J. Lu, M. Sabat and C. Fraser, *J. Am. Chem. Soc.*, 2010, **132**, 2160; (f) S. Yoon, J. Chung, J. Gierschner, K. Kim, M. Choi, D. Kim and S. Y. Park, *J. Am. Chem. Soc.*, 2010, **132**, 13675; (g) X. Luo, J. Li, C. Li, L. Heng, Y. Dong, Z. Liu, Z. Bo and B. Z. Tang, *Adv. Mater.*, 2011, **23**, 3261; (h) Z. Chi, X. Zhang, B. Xu, X. Zhou, C. Ma, Y. Zhang, S. Liu and J. Xu, *Chem. Soc. Rev.*, 2012, **41**, 3878; (i) N. Mizoshita, T. Tani and S. Inagaki, *Adv. Mater.*, 2012, **24**, 3350; (k) S. Yamane, Y. Sagara, T. Mutai, K. Araki and T. Kato, *J. Mater. Chem. C*, 2013, **1**, 2648.
- 3 (a) H. Rau, *Photochromism, Molecules and Systems*, ed. H. Dürr and H. Buuas-Laurent, Elsevier, Amsterdam, The Netherlands, 1990; (b) *Photoreactive Organic Thin Films*, ed. Z. Sekkat and W. Knoll, Academic Press, Elsevier Science, 2002; (c) H. Rau, *Angew. Chem. Int. Ed. Engl.*, 1973, **12**, 224; (d) C. G. Morgante and W. S. Struve, *Chem. Phys. Lett.*, 1979, **68**, 267; (e) J. Azuma, N. Tamai, A. Shishido and T. Ikeda, *Chem. Phys. Lett.*, 1998, **288**, 77; (f) H. Satzger, S. Sporlein, C. Root, J. Wachtveitl, W. Zinth and P. Gilch, *Chem. Phys. Lett.*, 2003, **372**, 216.
- 4 M. Nepraš, S. Luňák, R. Hrdina and J. Fabian, *Chem. Phys. Lett.*, 1989, **159**, 366.
- 5 (a) G. Gabor, Y. Frei, D. Gegiou, M. Kaganowich and E. Fisher, *Isr. J. Chem.*, 1967, **5**, 193; (b) H. Rau, *Ber. Bunsen-Ges. Phys. Chem.*, 1968, **72**, 1068.
- 6 H. Bisle and H. Rau, *Chem. Phys. Lett.*, 1975, **31**, 264.
- 7 (a) M. Ghedini, D. Pucci, G. Calogero and F. Barigelletti, *Chem. Phys. Lett.*, 1997, **267**, 341; (b) J. Yoshino, N. Kano and T. Kawashima, *Chem. Commun.*, 2007, 559.
- 8 (a) M. Shimomura and T. Kunitake, *J. Am. Chem. Soc.*, 1987, **109**, 5175; (b) K. Tsuda, G. C. Dol, T. Gensch, J. Hofkens, L. Latterini, J. W. Weener, E. W. Meijer and F. C. De Schryver, *J. Am. Chem. Soc.*, 2000, **122**, 3445; (c) H. Yu and L. Qi, *Langmuir*, 2009, **25**, 6781.
- 9 (a) M. Han and M. Hara, *J. Am. Chem. Soc.*, 2005, **127**, 10951; (b) M. Han, Y. Hirayama and M. Hara, *Chem. Mater.*, 2006, **18**, 2784; (c) P. Smitha and S. K. Asha, *J. Phys. Chem. B*, 2007, **111**, 6364; (d) B.-K. Tsai, C.-H. Chen and C.-H. Hung, *J. Mater. Chem.* 2012, **22**, 20874.
- 10 (a) J. Luo, Z. Xie, J. W. Y. Lam, L. Cheng, H. Chen, C. Qiu, H. S. Kwok, X. Zhan, Y. Liu, D. Zhu and B. Z. Tang, *Chem. Commun.*, 2001, 1740; (b) B.-K. An, S.-K. Kwon, S.-D. Jung and S. Y. Park, *J. Am. Chem. Soc.*, 2002, **124**, 14410; (c) S. Babu, S.; K. Kartha, A. Ajayaghosh, *J. Phys. Chem. Lett.*, 2010, **1**, 3413; (d) Y. Hong, J. Lam and B. Z. Tang, *B. Chem. Soc. Rev.*, 2011, **40**, 5361; (e) B. An, J. Gierschner and S. Y. Park, *Acc. Chem. Res.*, 2012, **45**, 544; (f) *Aggregation-Induced Emission*, ed. A. Qin and B. Z. Tang, Wiley, 2013.
- 11 (a) J. J. van Gorp, J. A. J. M. Vekemans and E. W. Meijer, *J. Am. Chem. Soc.*, 2002, **124**, 14759; (b) S. Ryu, S. Kim, J. Seo, Y. Kim, O. Kwon, D. Jang and S. Park, *Chem. Commun.*, 2004, 70; (c) C. Bao, R. Lu, M. Jin, P. Xue, C. Tan, T. Xu, G. Liu and Y. Zhao, *Chem.-Eur. J.*, 2006, **12**, 3287; (d) Y. Zhou, M. Xu, T. Yi, S. Xiao, Z. Zhou, F. Li and C. Huang, *Langmuir*, 2007, **23**, 202; (e) I. Danila, F. Riobe, F. Piron, J. Puigmarti-Luis, J. Wallis, M. Linares, H. Agren, D. Beljonne, D. Amabilino and N. Avarvari, *J. Am. Chem. Soc.*, 2011, **133**, 8344; (f) A. Bernet, R. Albuquerque, M. Behr, S. Hoffmann and H. Schmidt, *Soft Matter*, 2012, **8**, 66; (g) S. Cantekin, T. de Greef and A. Palmans, *Chem. Soc. Rev.*, 2012, **41**, 6125; (h) S. Lee, S. Oh, J. Lee, Y. Malpani, Y. Jung, B. Kang, J. Lee, K. Ozasa, T. Isoshima, S. Lee, M. Hara, D. Hashizume and J. Kim, *Langmuir*, 2013, **29**, 5869.
- 12 As mentioned in the introduction, fluorescence may occur from donor-acceptor substituted azobenzenes as well as from *o*- and *p*-hydroxy azo compounds. In particular, fluorescence from *o*- and *p*-hydroxy azo compounds is reported to be due not to the azo form, but rather to the tautomeric hydrazone form. However, we found no carbonyl stretching band in the infrared spectrum for fully dried **3N1** fibers (Fig. S5), implying that the red fluorescence emitted from the fibers is not likely due to the hydrazone form, but is due to the azo form.
- 13 M. Han, T. Honda, D. Ishikawa, E. Ito, M. Hara and Y. Norikane, *J. Mater. Chem.*, 2011, **21**, 4696.
- 14 (a) X. Song, J. Perlstein and D. Whitten, *J. Am. Chem. Soc.*, 1997, **119**, 9144; (b) I. Zebger, M. Rutloh, H. Hoffmann, J. Stumpe, H. W. Siesler and S. Hvilsted, *J. Phys. Chem. A*, 2002, **106**, 3454.
- 15 (a) L. B. McCusker, R. B. Von Dreele, D. E. Cox, D. Louër and P. Scardi, *J. Appl. Crystallogr.*, 1999, **32**, 36; (b) B. H. Toby, *J. Appl. Crystallogr.*, 2001, **34**, 210.
- 16 T. Hirade, Y. Okui and M. Han, *J. Mater. Chem. C*, 2013, **1**, 2672.
- 17 (a) M. Kasha, H. R. Rawls and M. Ashraf El-Bayoumi, *Pure Appl. Chem.*, 1965, **11**, 371; (b) F. Würthner, T. Kaiser and C. Saha-Möller, *Angew. Chem. Int. Ed.*, 2011, **50**, 3376.